Magnetic Field Complexity for Current-carrying Toroidal Coils

Katsuo Maxted

Physics Department, The College of Wooster, Wooster, Ohio 44691, USA

(Dated: May 11, 2011)

A simulation of magnetic field lines surrounding a current-carrying toroidal coil was created to understand their path complexity. The fields were first modeled through Mathematica to verify the accuracy of calculations, and then modeled through Xcode to effectively increase calculation speeds. By varying the initial position of a magnetic field path, regions of magnetic chaos around the winding loops of the current-carrying toroidal coil were observed.

I. INTRODUCTION

In the world of physics, It has always been known that magnetic fields of an ideal current-carrying toroidal coils have simple closed-loop paths. These are in shapes of circles or ellipses and can be located inside or outside a toroidal coil. But recently, **real** toroidal coils have been found to exhibit chaos. Aguirre et al found that chaotic magnetic fields exist in various current-carrying wire structures, with some resembling toroids.[1]

A. Background

In the past, unperturbed systems of straight currents and shaped loop currents were investigated, but there were no studies with perturbed systems that held similar configurations to currents of unperturbed systems.[1] Hosada, Miyaguchi, Imagawa, and Nakamura at the Osaka City University used simple wire configurations to exhibit erratic magnetic field behavior, showing that chaotic magnetic fields lines exist in simple and complex current-carrying wire structures. Examples of simple wire structures are straight and ring wires while complex wire structures include rippled ring wires, cross ring wires, and parallel-ring wires.[2]

A toroidal coil can be (crudely) diagnosed as what the Japanese researchers call a "rippled ring wire". Thus, an accurate hypothesis is that some realistic magnetic fields in or around a toroid are complex in nature, and cannot be easily predicted. No simulations on current-carrying toroids have ever been built, so it deserved investigation. It was uncertain if all of the magnetic fields generated by a current-carrying toroid are chaotic. There was a possibility that some regions could be simple and predictable, much like the magnetic fields of a current-carrying circle. To model the system and take qualitative data, it was critical to build a fast and accurate simulation.

B. Coding Techniques

Two programs, Mathematica and Xcode, were used to simulate a current-carrying toroid with a surrounding magnetic field.

1. Mathematica Coding

An advantage of Mathematica is that it is pre-coded with mathematical methods, making the input of commands more intuitive. It essentially works as an advanced graphing calculator. The main disadvantage to using a numerical solver like Mathematica is that the calculation speeds are slow when compared to hard code that only uses necessary commands.

2. Xcode Coding

Xcode is a major benefit for simulated experiments that require massive data-taking. Since the entire simulation can be written from scratch, experiments can be designed strictly to the customary needs of the tester. The disadvantage is, of course, the amount of required coding is much longer than whats asked from a numerical solver. This means the tester must have the focus to program over a long period and experience in programming languages such as C, C++, objective-C, and objective-C++.

II. THEORY

One common misunderstanding of magnetic field lines is that they are "roads" that magnetic monopoles, if they existed, would follow. Though magnetic monopoles never have been proven to exist, they would essentially follow the behavior that electric charges have with electric fields. Thus, magnetic monopoles should not be able to travel along the magnetic field lines. In a case where a magnetic monopole is introduced in the system, if it is moving through a magnetic field with an initial velocity, its acceleration, not the velocity, is always parallel to the direction of the magnetic field lines. Note that the magnetic field lines are merely **influences** that can affect the velocity of a monopole.

A. Toroid Geometry

Before delving into the physics of the magnetic fields, the geometry of the toroid had to be fully understood.
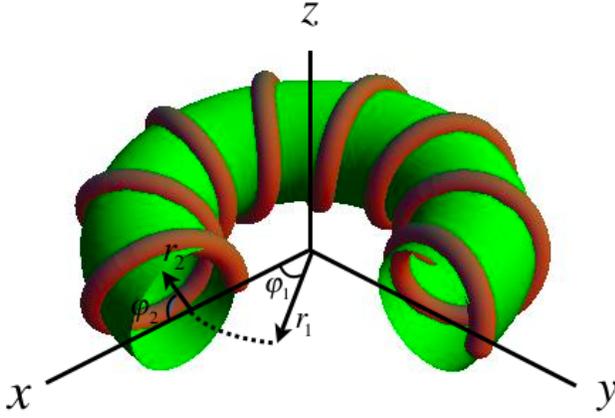
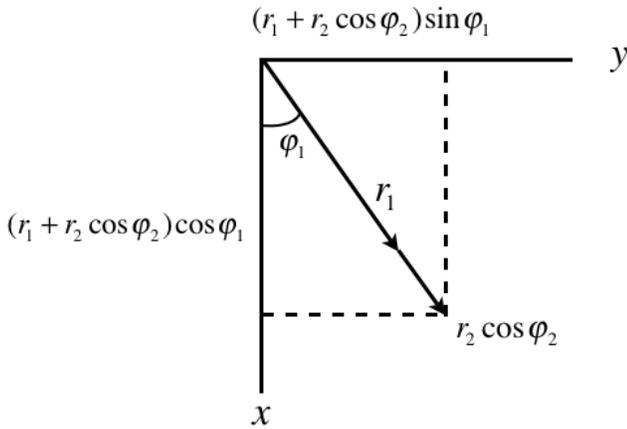FIG. 1: The three-dimensional cross section of a toroid with an imaginary torus inside.

FIG. 2: A diagram of the components of $\vec{r}$. $r_1 + r_2 \cos \phi_2$ is the projection of $\vec{r}$.

It was necessary to compose a vector that began at the origin or center of the toroid and ended at a point on the current-carrying coil. If this vector of interest is called $\vec{r}$, it can be the sum of a vector extending from the origin to the center of a winding loop and a vector extending from the center of a winding loop to a point on the coil. This is simply expressed as $\vec{r} = \vec{r_1} + \vec{r_2}$ The geometry given in Fig. 1 and Fig. 2 show that

$$\vec{r} = \{(r_1 + r_2 \cos \phi_2) \cos \phi_1, (r_1 + r_2 \cos \phi_2) \sin \phi_1, r_2 \sin \phi_2\} \tag{1}$$

ϕ_1 is proportional to the number of poloidal windings n_p and ϕ_2 is proportional to the number of toroidal windings n_t. The poloidal direction is defined as the direction through the bottom and top of the coil, and the toroidal direction is defined as the direction perpendicular to the poloidal direction. ϕ_1 and ϕ_2 are derived to be $\phi_1 = n_1 \phi$ and $\phi_2 = n_2 \phi$.
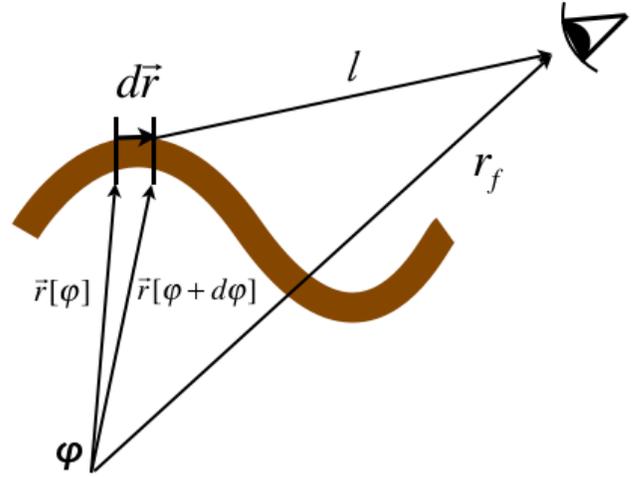

FIG. 3: Diagram of the orientation of vectors that compose the position of a point on a magnetic field.

B. Biot-Savart

Assuming that there is a current running through the coil, to calculate a magnetic field line at a distance from the coil, it is necessary to step along the wire to calculate points that are on the magnetic field line. The direction of each step is always tangent to the toroid's wire curve. This is equal to

$$d\vec{r} = \vec{r}[\phi + d\phi] - \vec{r}[\phi] = \frac{d\vec{r}}{d\phi} d\phi \tag{2}$$

because $\vec{r}[\phi]$ is rotated by $d\phi$ for one $d\vec{r}$. The magnetic field needs to be calculated for a unique point in space that is not on the coil. A vector $\vec{l}$ that reaches from the end of $d\vec{r}$ to the unique point in space from a point on the coil can be given as

$$\vec{l} = \vec{r}_f - \vec{r}[\phi + d\phi], \tag{3}$$

where $\vec{r}_f$ is a vector that extends from the origin or center of the toroid to the unique point in space. A schematic is shown in Fig. 3. The magnetic field vector can be found using the Biot-Savart Law:

$$\vec{B} = \frac{I}{4\pi} \int_{\phi=0}^{2\pi} \frac{d\vec{r}}{d\phi} d\phi \times \frac{\hat{l}}{l^2}. \tag{4}$$

This is used to integrate for the x, y and z components of $\vec{B}$.[3] The current is denoted as I and $d\vec{r}$ is used as the variable of integration because the law requires integration through steps that are tangent to the curve of the coil. Note that $\hat{l}/l^2 = \vec{l}/l^3$ because the unit vector $\hat{l}$ is the vector $\vec{l}$ divided by the magnitude l.
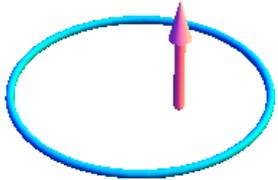
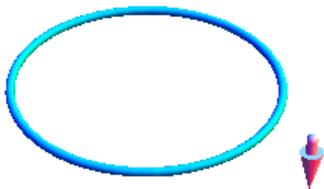FIG. 4: A magnetic vector $\vec{B}$ pointing upward through a circle loop where $n_t = 0$.

FIG. 5: A magnetic vector $\vec{B}$ pointing downward beside a circle loop where $n_t = 0$.
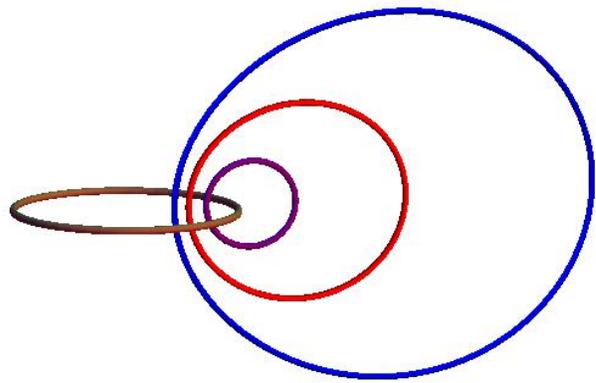

FIG. 6: Three magnetic field lines about a circle loop with different initial x (x_0) positions. The three magnetic field loops are located on the same two-dimensional xz plane.
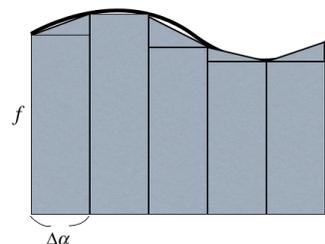

FIG. 7: An illustration of how the trapezoidal rule is implemented when integrating the function $f[\alpha]$. When the refinement number is increased, the trapezoids under the curve become more narrow. Though this increases the accuracy of the integration, the calculation time rises exponentially.

III.   SIMULATION

First, I modeled the magnetic field lines in Mathematica before collecting high-speed data. A three-dimensional parametric plot was used to model a toroidal coil carrying a current.

Using Eq. (4), the integrand was derived and integrated from 0 to 2π for each x, y, and z component. Even with an indefinite integral, Mathematica failed to provide an answer. Thus, I used numerical integration to obtain decimal values of points positioned on the magnetic field. The path of the magnetic field lines was completely unknown so it was necessary to verify that the numerical integration was providing accurate values. This was checked by printing clips of a magnetic vector around a circle loop. A current-carrying circle loop was used because it was known to generate simple, circular magnetic field paths. Fig. 4 and Fig. 5 show a magnetic field vector inside and outside a current loop with $n_t = 0$. Next, three magnetic field loops with three different initial distances were drawn about one point on the current loop. As x_0 approaches closer to the current loop, the magnetic field loop gets smaller. This is shown in Fig. 6. After verifying that Mathematica displayed convergence into accurate results, Xcode programming was commenced. The purpose of this was to make calculations run quicker, for the time for Mathematica calculations ranged from 5 to 12 hours. As it was crucial to find trends in the magnetic field line behavior, fast calculations were highly effective for this research. The integration was looped n times, with n being the number of times the integral is calculated. The Trapezoidal Rule was used as the technique for integration.

A.   Trapezoidal Rule

The trapezoidal rule was used to numerically integrate in Xcode. The trapezoidal rule provides the area of trapezoids under the graph of the function $f[\alpha]$, which is given in Fig. 7. The area can be divided into multiple trapezoids, and the area of one trapezoid is $((b+t)/2)\Delta\alpha$ where b is the base of the trapezoid, t is the top of the trapezoid, and α is the distance between b and t. In this study, the area under the function $\partial B/\partial \alpha$ was found. A variable called the refinement number was used to shorten or lengthen the trapezoid heights. A large refinement number allowed convergence to an accurate magnetic field. The sum of the area of multiple trapezoids can be expressed as

$$B_{x,y,z} = \frac{f_0 + f_1}{2}\Delta\alpha + \frac{f_1 + f_2}{2}\Delta\alpha + \frac{f_2 + f_3}{2}\Delta\alpha + ... + \frac{f_{n-1} + f_n}{2}\Delta\alpha, \tag{5}$$

which can be simplified to

$$B_{x,y,z} = \Delta\alpha \left(\frac{f_0}{2} + f_1 + f_2 + f_3 + ... + \frac{f_n}{2} \right). \tag{6}$$

$B_{x,y,z}$ denotes that the trapezoidal rule was used for the x, y, and z components. It was clear that as the integration refinement number was increased and the integration length step was decreased, a magnetic field would converge to a set shape.

B. Experiment

Qualitative analysis showed that there are very complex magnetic field lines around and in the toroidal windings. It was decided that these areas of high complexity deserved further investigation. Fig. 8 shows the interface that was used to manipulate the simulation. Two parameters were varied during my simulated experiments. One was the initial position of x_0 and the other was the toroidal winding number n_t. Using a fixed r_1, r_2, and n_p, the winding number was varied to find how it affects the complexity of chaotic regions. For each winding number, the starting location x_0 was moved from the center to inside the winding loops to find how the magnetic field complexity changes.

For all of my trials, the initial positions of y_0 and z_0 remained at one. The values for all initial positions had to be non-zero because otherwise the results for the numerical integration would diverge. The reason for the divergence is unknown, but a possible related fact is the magnetic field at the origin or center of a current loop is a straight line that extends to ∞ and $-\infty$ in the z and $-z$ directions.

IV. ANALYSIS & RESULTS

Fig. 9 shows that chaotic magnetic field lines always display circular or spiraling characteristics. From the center of the toroid, as x_0 approaches closer to the toroidal windings, the magnetic field would increase in complexity. Near the origin, the magnetic field displays
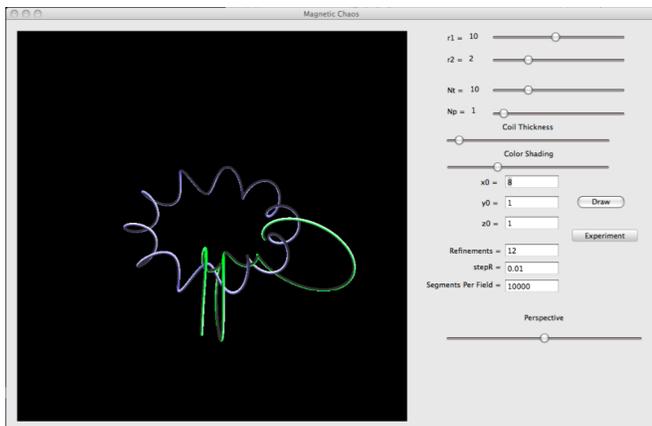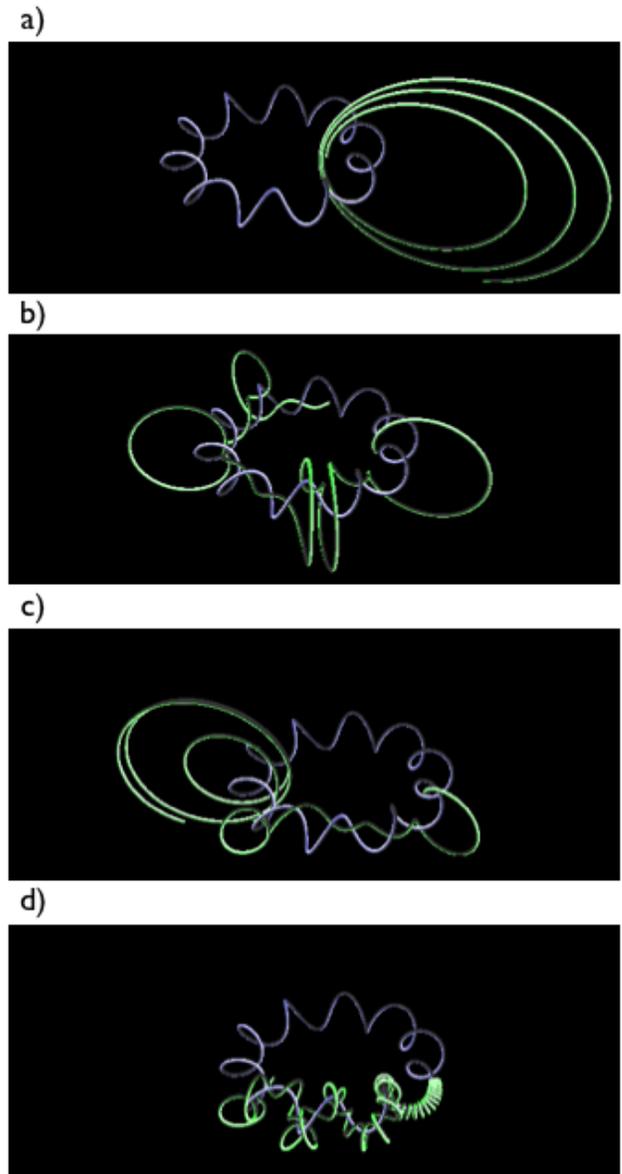

FIG. 9: a, b, c, d show the magnetic fields from x_0 in the order of 6.0, 8.0, 10.0, and 12.0. As the initial position approaches the wire, the magnetic field complexity increases.
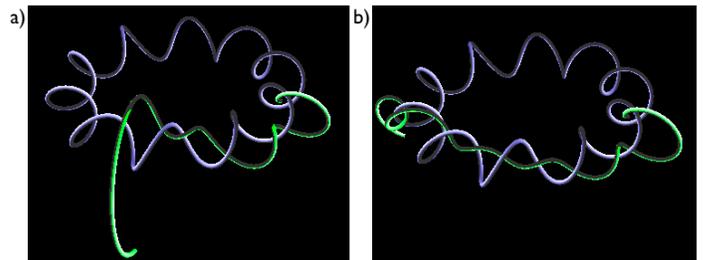

FIG. 10: a, b display a magnetic field that is sensitive to slight changes in initial conditions. a has an x_0 of 10.5, which is decreased by 0.1 for b. The coil has an n_t of 10.

FIG. 8: A picture of the Xcode interface that was used to perform simulations.
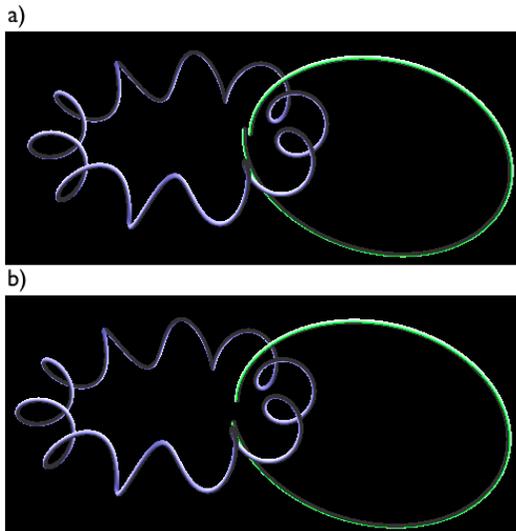
a)

b)

FIG. 11: a, b display a magnetic field that has little sensitivity to slight changes in initial conditions. a has an x_0 of 6.0, which is increased by 0.1 for b. The coil has an n_t of 10.

simple elliptical shape that loops around the coil few times. But as x_0 approaches the wire, the magnetic field exhibits an increasingly complicated structure with many loops. When x_0 is very close to the toroid, as in Fig. 10, the field is extremely sensitive to slight changes of the initial positions. As a result, the region that this field is in can be considered chaotic. But in Fig. 11, when x_0 is farther from the wire, the field exhibits little sensitivity to the same change of x_0. This region can be considered as anti-chaotic. Anti-chaotic is defined as structurally simplistic but not predictable. With the same x_0 change of 0.1, Fig. 10 and 11 showed a large difference in field sensitivity. Fig. 9, 10, 11 used constant parameters of $n_t = 10$, field segments = 10000, refinement number = 12, and $dt = 0.01$. A refinement number of 12 was used because it was the lowest value that displayed complete field convergence for all simulations.

V.   CONCLUSIONS

While a high number of refinements provides accurate field values, the graph of the calculation time vs. refinement number clearly shows that calculations are significantly slower. There is a linear relationship between the calculation time vs. the segments per magnetic field number. The complexity of a magnetic field line is inversely proportional to the distance from the winding loops to a point closer to the origin. Field sensitivity is high when x_0 is close to the wire, but is low when x_0 is close to the origin.

VI.   ACKNOWLEDGEMENTS

[1] J. Aguirre and D. Peralta-Salas, *Euro. Phys. Lett.* 80, 60007 (2007).

[2] M. Hosada, T. Miyaguchi, K. Imagawa, and K. Nakamura, *Phys. Rev. E.* 80, 067202 (2009).

[3] J. Aguirre, J. Gine, and D. Peralta-Salas, *Nonlinearity* 21, 51 (2008).